Electronic structure of rare-earth nickel pnictides: Narrow-gap thermoelectric materials

P. Larson and S. D. Mahanti
Department of Physics and Astronomy, Michigan State University, East Lansing, Michigan 48824

Sandrine Sportouch and M. G. Kanatzidis
Department of Chemistry, Michigan State University, East Lansing, Michigan 48824

(Received 16 November 1998)

We have studied the electronic structure of a class of half-Heusler compounds MNiPn, where M is Y, La, Lu, Yb, and Pn is a pnicogen As, Sb, Bi. All these systems excepting Yb are narrow-gap semiconductors and are potential candidates for high-performance thermoelectric materials. The Yb system shows heavy fermion characteristics. Calculations were carried out within density-functional theory (generalized gradient approximation) using self-consistent full-potential linearized augmented plane-wave method. Comparison of the electronic structures of isoelectronic systems YNiSb and ZrNiSn, another narrow-gap semiconductor, brings out the role of hybridization on the energy gap formation. We also find that in YNiPn systems, the gap narrows as we go from As to Bi, a result of relativistic lowering of the Pn valence *s* band and its influence on the lowest conduction band. Our band-structure results for YbNiSb differs drastically from a previous calculation using a different method, but agrees closely with a similar mixed valence system YbPtBi. [S0163-1829(99)03324-X]

I. INTRODUCTION

A deeper understanding of the electronic structure of multinary compounds with complex structure has become extremely important both from a fundamental and materials science points of view. Such materials are being synthesized with a view to enhancing thermoelectric, magnetic, piezoelectric, and other material characteristics. A class of compounds that has attracted a great deal of attention in recent years is that with the MgAgAs-type structure. Examples of such systems are: MNiSn (M=Ti, Zr, Hf, U, Th);[1–3] MNiSb (M=Y, Gd, Yb, Lu);[4–6] and MPtBi (M=Yb).[7,8] These systems can be either metals or semiconductors. In fact some of the metallic systems show heavy fermion characteristics,[7,8] while others are promising candidates for high-performance thermoelectric materials. For example, a few years ago the ternary intermetallic compounds MNiSn (M=Ti, Zr, Hf) were reported to exhibit unusual transport and optical properties expected from semiconductors. Indeed, they were later established to be narrow-gap semiconductors.[1,2] A remarkable feature of these materials is that, despite the fact that they are composed of only metallic elements, they are semiconductors. The origin of gap formation in these systems is therefore an interesting and subtle issue.[2]

Recently, we have initiated investigations on the potential of the ternary phases of the MgAgAs structure type for thermoelectric applications. We are particularly interested in the electronic properties of $M^{3+}NiPn^{3-}$-type phases, where M is a trivalent electropositive element and *Pn* is a pnicogen element, and various derivatives thereof. These compounds are isoelectronic to the MNiSn phases discussed above,[1–3] and in this respect they represent a logical new direction for thermoelectric investigations.[9] The $M^{3+}NiPn^{3-}$ compounds crystallize in the cubic MgAgAs structure type, see Fig. 1; where the electropositive metals occupy the Mg sites while the Pn occupies the As site. This structure can be described as a filled MgAs, NaCl structure type in which Ag atoms are inserted in half of the tetrahedral holes in the lattice. In this description, the compounds can be viewed as complexes of guest Ni atoms in the host $M^{3+}Pn^{3-}$ lattice. An alternate way to describe the $M^{3+}NiPn^{3-}$ is to consider this compound as a filled adamantane $[AgAs]^{3-}$, ZnS zinc-blend-type lattice in which the Mg^{2+} atoms occupy octahedral holes in a diamond lattice. In either case, the cubic cell has unfilled holes that present the opportunity for chemical experimentation.

In this paper, we discuss the electronic structure of systems where M=Y, La, Yb, and Lu and X=Sb, As, Bi. Our main motivations for undertaking this study are: (i) to see how the element M determines whether the system is a metal or a semiconductor as seen in some experiments, (ii) if it is a semiconductor, what is the physical origin of the energy gap formation and how does this gap depend on M and X, and (iii) to explore the role of the *f* electrons on the electronic structure in general.[10] Furthermore, a recently published electronic structure calculation[4] in YbNiSb using linear muffin-tin orbital (LMTO) method in the atomic sphere approximation (ASA) within the local-density approximation is found to differ drastically from that of YbPtBi,[7] a very similar system. This is quite surprising and we felt it was important to redo the calculations in YbNiSb using a different

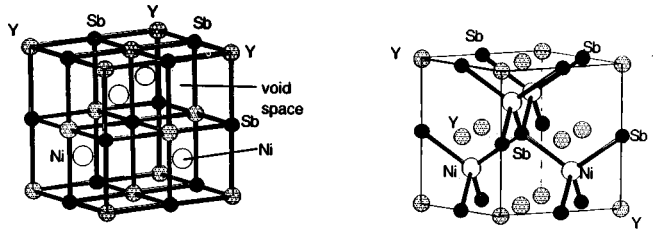

FIG. 1. Two different perspectives of the cubic structure of YNiSb. Left: Ni atoms inserted in a YSb NaCl-type lattice. Right: Y atoms inserted in a ZnS-type NiSb lattice.

TABLE I. Lattice constants and band gap.

System	Lattice Constant a (a.u.)	Calculated Band Gap (eV)
YNiSb	11.928	0.28
LaNiSb (cubic)	12.603	0.44
LuNiSb	11.752	0.19
YbNiSb	11.788	Metal
LaNiSb (hexagonal)	$a=8.353$	Metal
	$c=15.585$	
YNiAs	11.662	0.53
YNiBi	12.115	0.13

method to clarify this issue. For purposes of comparison and to understand the physical reason behind the energy-gap formation at the Fermi level, we have also calculated the band structures of the ''host'' binary materials MSb ($M=$Y, La, Lu, Yb) and explored how the behavior of bands near the Fermi energy change as we go from MSb to MNiSb in terms of orbital interactions with the inserted Ni atoms.

The organization of the paper is as follows: In Sec. II, we discuss the crystal structure of these compounds and describe very briefly the method we have used to calculate the electronic structure. In Sec. III, we present our results and in Sec. IV, we summarize and discuss the adequacy of the local-density approximation (and improvements beyond LDA) in describing the electronic structure of systems containing f electrons. In this context, we review a recent work on a similar system, namely YbPtBi.[7]

II. CRYSTAL STRUCTURE AND METHOD

MNiSb compounds formed with light rare-earth elements (M) crystallize with a hexagonal ZrBeSi structure (Space group: P 6_3/mmc) whereas those with Yttrium and heavy rare earths crystallize in the cubic MgAgAs structure (Space group: F 43m). In this paper we deal with the latter structure, but for the sake of comparison with compounds having cubic structure we have also considered a hypothetical LaNiSb compound with cubic structure. In Table I, we give the lattice constants used in the present study.

The noncentrosymmetric crystal structure of MNiSb ($M=$Y) is shown in Fig. 1. As discussed before, this system can be viewed as a rock-salt structure arrangement of M and Sb atoms with Ni atoms occupying the center of cubes formed by four M and four Sb atoms. Actually, there are two such cube-center positions which the Ni atoms can occupy, but in the MNiSb compounds only one of the cube-center positions (also forming an fcc lattice) is occupied by the Ni atoms. On the other hand, in metallic Heusler compounds MNi$_2$Sb, all cube-center positions are occupied by Ni atoms and the system recovers the center of inversion.[11] In both these systems each Ni atom bonds with four M and four Sb nearest-neighbor atoms. We will later argue that Ni plays a very important role in the final band structure of these systems.

Electronic structures were calculated using self-consistent full-potential linearized augmented plane-wave (LAPW) method[12] within density-functional theory[13] (DFT) using the generalized gradient approximation (GGA) of Perdew, Burke, and Ernzerhof[14] for the exchange and correlation potential. The calculations were performed using the WIEN97 package.[15] The values of atomic radii were taken from Pauling's table [L. Pauling, J. Am. Chem. Soc. **69**, 542 (1947)]. They are 2.18 a.u. for Ni and are 2.36 a.u. for As, Sb, and Bi. The atomic radii for the rare earths were kept constant at 2.46 a.u., close to the value for Y. Adjustment of these radii within a reasonable range showed little dependence of the final band structure on these variations. Convergence of the self-consistent iterations was performed with 22 **k** points in the reduced Brillouin zone to within 0.0001 Ry with a cutoff between valence and core states of -6.0 Ry. Relativistic corrections were incorporated in two stages. Scalar relativistic corrections were added for all the systems studied and spin-orbit (SO) interactions were included using a second variational procedure.[16] The latter is particularly significant for the f electrons and for heavy atoms such as Bi. For all the systems, we have calculated the band structure with and without the SO corrections and find that the inclusion of SO interaction has a significant effect on the states near the Fermi energy for a large number of systems of interest. All the results reported in this paper include SO interaction.

III. RESULTS

A. YSb, LaSb, YbSb (model systems for comparison)

Before discussing the band structure of systems containing Ni, let us see the nature of the electronic structure for MSb ($M=$Y, La, Yb) which has the NaCl structure. In Figs. 2(a), 2(b), and 2(c) we give their band structures and in Figs. 3(a), 3(b), and 3(c) we give the corresponding total density of states (TDOS), both of which suggest that all three systems are metals. Our results for YSb and LaSb agree qualitatively with an earlier calculation (LDA and no spin-orbit interaction) using a self-consistent APW procedure by Hasegawa.[17] In these two systems, the lowest three bands shown of Figs. 2(a) and 2(b) are weakly hybridized Sb-p and M-d bands, although they have predominantly Sb p character. We will for the sake of argument refer to these three bands as the ''valence'' bands. Both in our and Hasegawa's calculations, an important feature is the existence of a band that lies just above these ''valence'' bands. In YSb for example, it starts from the Γ point (has Γ_{25} symmetry), drops dramatically as one moves towards the X point (X_3 symmetry) and then rises along XW. A detailed analysis of the orbital character reveals that this band is primarily of Y $4d$ character and is a characteristic feature in the NaCl crystal structure type.[3] Because this band comes down appreciably and falls below the top of the valence band, which is at the Γ point, the system behaves like a semimetal with pockets of holes around the Γ point and pockets of electrons around the X point. In LaSb and LuSb (not shown in the figure), the presence of empty f orbitals above the Fermi level and completely filled f levels below the Fermi level, respectively, do not change this basic semimetallic behavior. However, there is some reordering of energy levels near the X point resulting from weak f-p and f-d hybridization. On the other hand, in YbSb [Fig. 2(c)], the Yb f levels lie at the Fermi level and hybridize strongly with the Sb p band. At the same time the Yb d bands get pushed above the Fermi energy.

Before discussing the results for systems with Ni, we would like to make two points. Our calculated density of

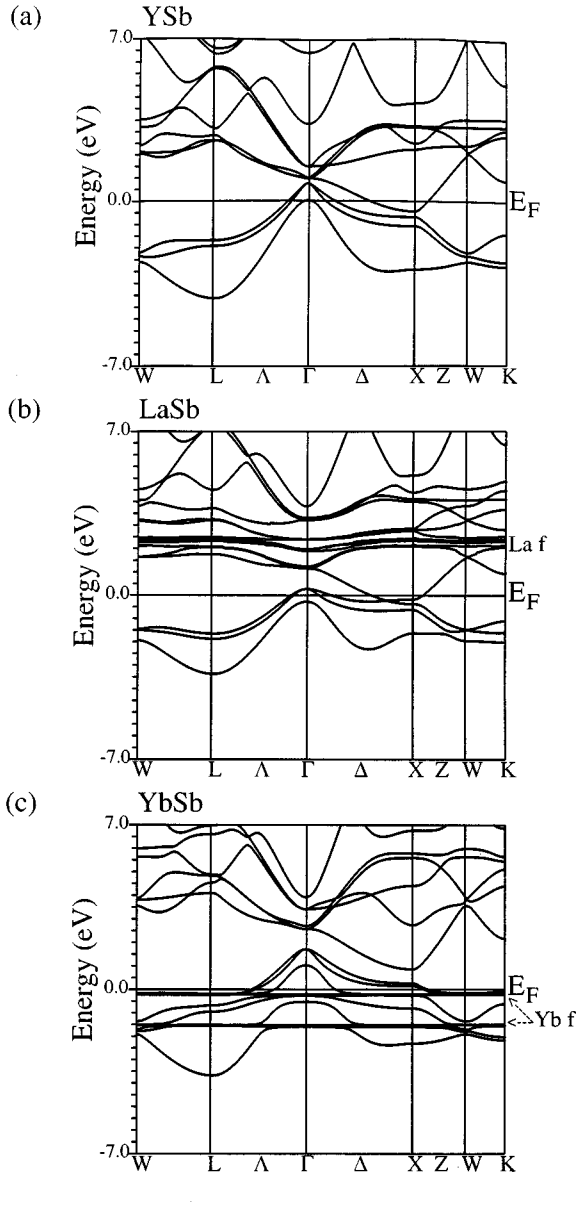

FIG. 2. Band structure of YSb (a), LaSb (b), YbSb (c).

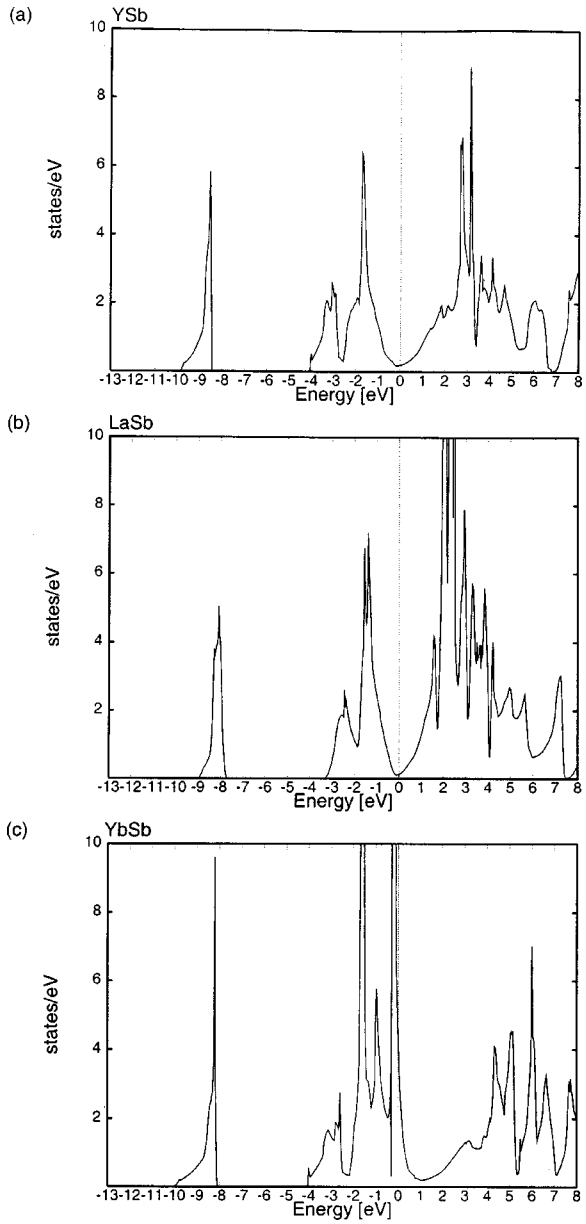

FIG. 3. Total density of states of YSb (a), LaSb (b), YbSb (bottom). The position of the Fermi energy is at zero energy.

states (per formula unit) at the Fermi energy using GGA for YSb and LaSb are 0.19 states/eV and 0.12 states/eV, respectively (see Fig. 3) These are about a factor of 2.5-3 smaller than earlier LDA results of Hasegawa.[17] A detail comparison between results obtained with LDA and GGA (with and without SO interactions) and the importance of electron-phonon contributions to the low-temperature electronic heat capacity in these systems will be discussed in a subsequent publication.

B. YNiSb, LaNiSb (both cubic and hexagonal), LuNiSb

Let us now analyze the effect of inserting Ni atoms into the MSb systems. As discussed before, MNiSb compounds have the MgAgAs-type structure (except for the case where $M=$La, where we will consider both the hexagonal and a hypothetical cubic structure) with M in 4(a): (0, 0, 0), Ni in 4(d): $(\frac{3}{4}, \frac{3}{4}, \frac{3}{4})$, and Sb in 4(b): $(\frac{1}{2}, \frac{1}{2}, \frac{1}{2})$ Wycoff positions. The position of 4(c): $(\frac{1}{4}, \frac{1}{4}, \frac{1}{4})$ is empty. The band structures for YNiSb, LuNiSb and LaNiSb (both cubic and hexagonal) are given in Figs. 4(a), 4(b), 4(c), and 4(d), respectively. As can be seen in all four cases, most of the Ni d bands lie below the Fermi level (about 1 to 3 eV below). However the lowest conduction band along Γ-X-W has appreciable Ni d-character. The Ni 4s bands are found considerably above the Fermi level, making Ni an almost d (Ref. 10) system. In addition, the Ni d orbitals interact strongly with the M d orbitals. In particular the X_3 state at the X point in YSb gets pushed sufficiently up and now lies above the Fermi energy. This opens up an energy gap and makes these systems indirect narrow gap semiconductors. A similar situation also occurs in the La and Lu systems. This opening of a gap was also seen in MNiSn systems by Ogut and Rabe,[2] which contain no f electrons. Since the f levels in the La and Lu systems lie more than 3 eV above and about 5 eV below the

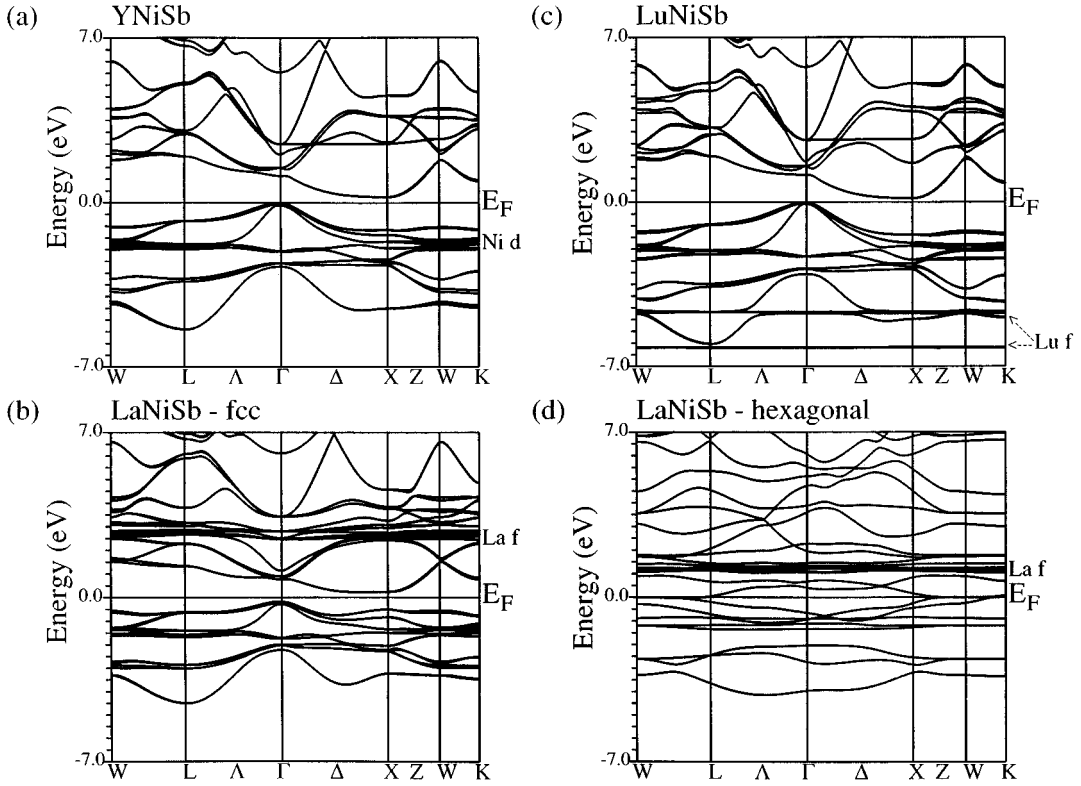

FIG. 4. Band structure of YNiSb (a), cubic LaNiSb (b), hexagonal LaNiSb (d), LuNiSb. The Ni *d* bands are explicitly shown in (a) and lie roughly in the same range in other three systems.

Fermi level, respectively, the *f*-*p* hybridization does not significantly affect the band structure in the neighborhood of the Fermi level. Thus, the origin of the gap formation in MNiSb ($M \neq$ Yb) compounds must be due to the insertion of Ni *d* orbitals, as in the case of MNiSn, although the particular details may differ somewhat. This point will be discussed more extensively later in the paper.

As has been pointed out in the introduction, MNiSb compounds with light rare-earth elements actually form in a hexagonal structure. We have, therefore; carried out a calculation of the electronic structure of hexagonal LaNiSb [see Fig. 4(d)]. As can be seen from the band structure, this system is a metal and its band structure differs significantly from the corresponding cubic system. A rather noticeable feature in the hexagonal compound is that the partly empty *f* levels (at ~1.5 eV) come closer to the Fermi energy.

C. YbNiSb

The Yb atom has one hole in the *f* shell and the compound is most likely a mixed valence heavy-fermion system.[5] Here, we are interested to see how well one can apply standard *ab initio* band-structure calculations based on density-functional theory to obtain a realistic description of the electronic structure near the Fermi energy. Similar attempts have been made successfully by Runge *et al.* for the mixed valence systems $CeRu_2Si_2$.[18] Of course one has to be careful in comparing the results of band calculations (within DFT) with experiments for systems where the *f* levels lie at the Fermi energy. This point will be discussed later in the paper.

The only published electronic structure calculation for

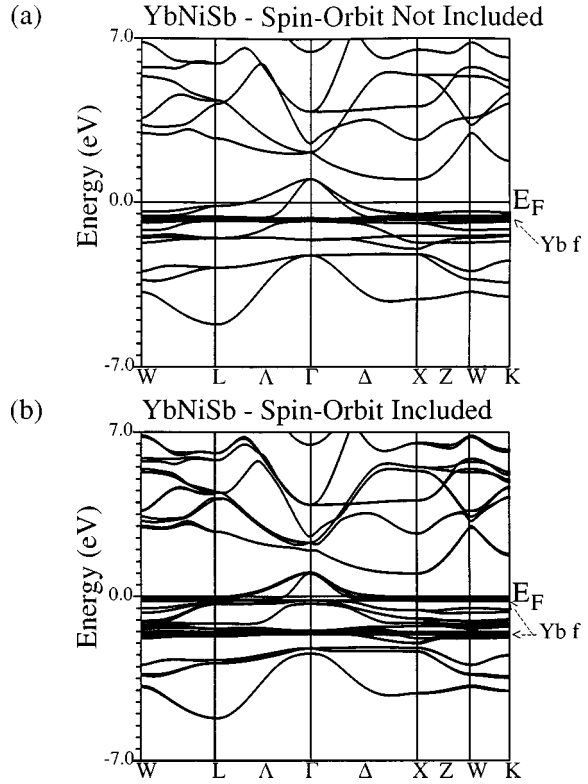

FIG. 5. Band structure of YbNiSb without (a) and with (b) spin-orbit interaction. The *f* levels split by about 1.25 eV.

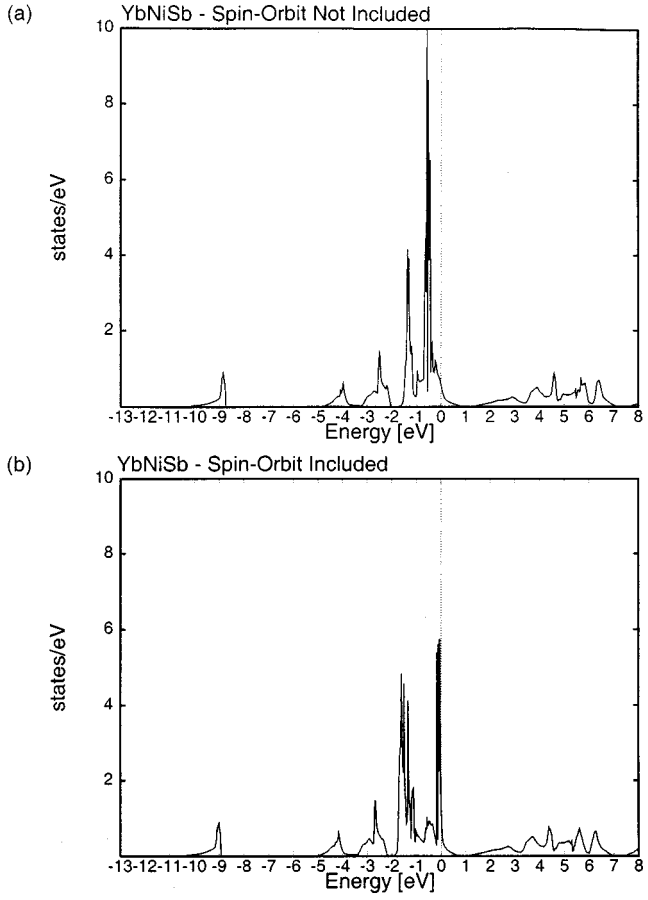

FIG. 6. Total density of states of YbNiSb without (a) and with (b) spin-orbit interaction.

YbNiSb of which we are aware of is by Solanki *et al.*[4] and it was carried out at the scalar relativistic level within LDA using LMTO-ASA. Unfortunately, their result differs considerably from that of the closely related system, YbPtBi, obtained by McMullen and Roy.[7] Also the calculated band structure in Ref. 4 appears strange with several flat portions. We, therefore, decided to redo the calculations for YbNiSb using a different method, namely full potential LAPW and using GGA, which improves over LDA by incorporating gradient corrections and is expected to be better for systems where the narrow *f* levels come close to the Fermi energy.

In Figs. 5(a) and 5(b) we give the band structure of YbNiSb without and with SO interaction and in Figs. 6(a) and 6(b) we give the corresponding total density of states, TDOS. The SO interaction is quite strong for the *f* levels and the splitting between $f_{5/2}$ and $f_{7/2}$ levels is about 1.25 eV, in agreement with the calculations on YbPtBi.[7] In YbSb, we found that there was a strong *f*-*p* hybridization near the Fermi level although the majority of the *f* levels were below the Fermi level. Insertion of Ni in the lattice (to form YbNiSb) places the Ni *d* bands below the *f* levels, which get pushed up in energy. As a result, there is a partial charge flow from the Yb *f* levels into the Sb *p* bands. Yb *f* levels become partially occupied and YbNiSb acquires a heavy fermion character much like YbPtBi. The DOS shows a substantial *f* character at the Fermi energy. The TDOS at the Fermi level, $N(\epsilon_F)$, is 12.6 states/eV of which 77% is of

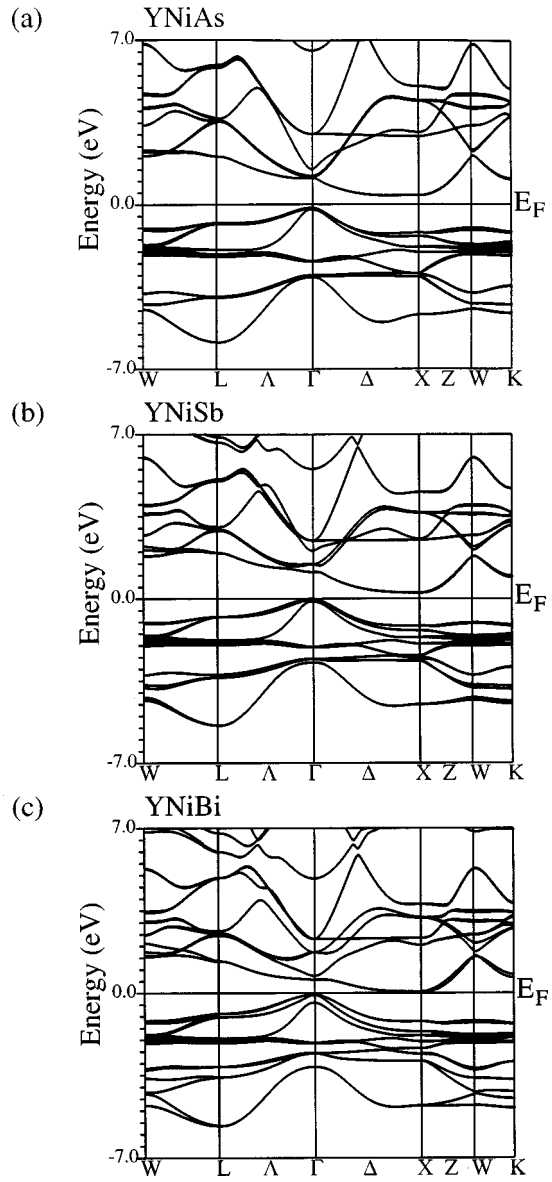

FIG. 7. Band structure of YbNiAs (a), YNiSb (b), and YNiBi (c). The indirect gap is seen to decrease as one goes from As to Bi.

Yb *f* character. In comparison, the corresponding numbers for YbPtBi are 4.5 states/eV and 60%, respectively.[7] It should be emphasized that if we do not include the SO interaction, $N(\epsilon_F)$ reduces to about 6.9 states/eV and the *f* character also gets reduced to 61%. Therefore, SO interaction should play an important role on the low-energy properties (the linear term in the heat capacity and the transport properties) of the system. To ascertain whether or not the difference in our results and those of Solanki *et al.*[4] are due to the two different methods (LMTO-ASA and FP-LAPW) and two different approximations (LDA and GGA), we calculated the band structure of YbPtBi using our procedure and our results agree rather well with those of McMullen and Roy,[7] who have used LMTO-ASA and LDA.

D. YNiPn (Pn=As, Sb, Bi)

In Figs. 7(a), 7(b), and 7(c) we give the band structures of YNiAs, YNiSb, and YNiBi to illustrate the effect of chang-

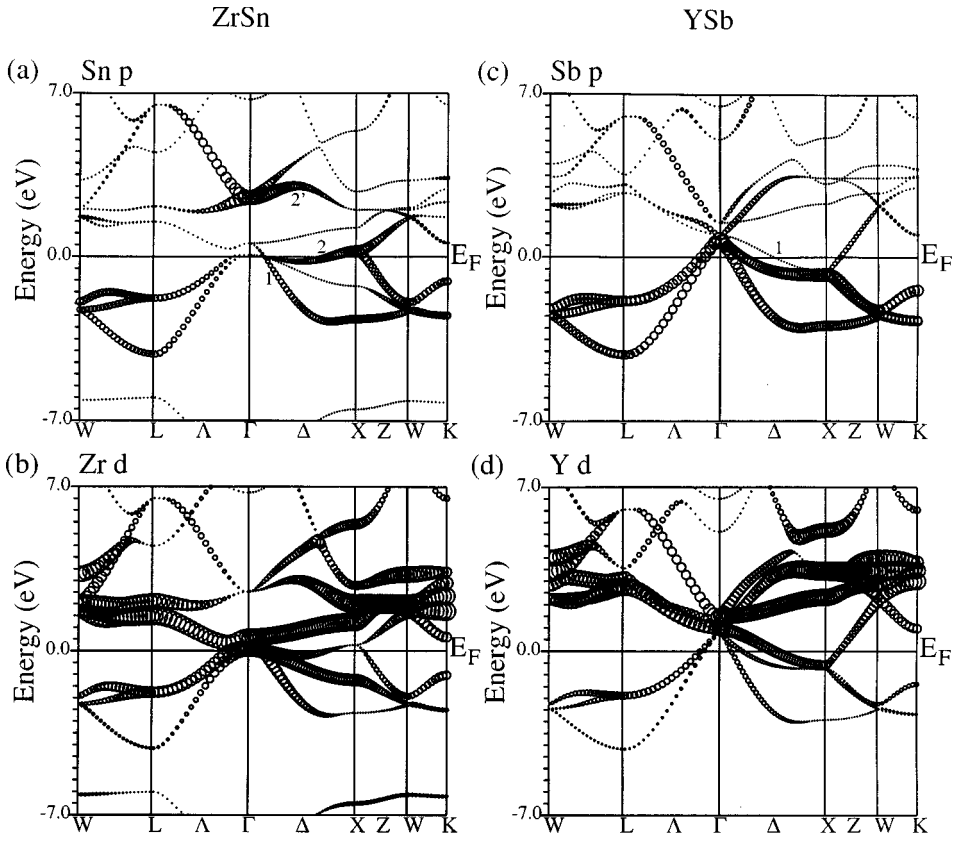

FIG. 8. Comparison of different angular characters and p-d hybridization between the parent compounds ZrSn (a) and (b) and YSb (c) and (d). The size of the circles is a measure of the angular characters. Figures 8(a) and 8(c) give the p characters of Sn and Sb and Figs. 8(b) and 8(d) give the d characters of Zr and Y, respectively.

ing the pnictogen atom on the energy gap. Clearly, the relativistic effects increase in going from As to Bi. In addition to the increase in spin orbit splitting we find that the Pn valence s band comes down towards the Fermi level and in Bi compounds it strongly perturbs the lowest conduction band (along the ΓX direction). The net effect is a decrease in the indirect band gap in going from As to Bi. The calculated band gaps are 0.53, 0.25, and 0.13 eV, respectively (see Table I where the band gaps for all the systems studied in this paper are given).

E. Origin of the gap formation

Finally, we would like to discuss the similarities and differences in the origin of the energy gap formation in ZrNiSn and YNiSb. These two systems are ideal for comparison because (Zr, Y) and (Sn, Sb) are neighboring pairs in the periodic table. In particular, we are interested in exploring the significance of (i) Zr (Y) d and Sn (Sb) p hybridization, and (ii) the Ni d orbitals on the electronic structure near the Fermi energy. Ogut and Rabe[2] have pointed out the important role played by p-d hybridization along the ΓX direction on the energy gap formation in ZrNiSn. They argued that the strong **k**-dependent hybridization between Zr d_{xz} and d_{yz} and Sn p and p_y along (001) direction was one of the two reasons behind the gap formation at the Fermi energy. In Figs. 8(a) and 8(b) we give the results of our FLAPW—GGA calculations for the host system ZrSn. They show the Sn p (a) and Zr d characters (b), the strengths of the orbital character being proportional to the size of the circles. The band labeled $2'$ starts out with Sn p character at the Γ point and changes over to Zr d character at the X point. The band labeled 2 shows just the opposite behavior. Clearly, there is evidence of strong **k** dependent p-d hybridization between the bands labeled 2 and $2'$ [shown in Fig. 8(a) and the corresponding bands in Fig. 8(b)] as pointed out by Ogut and Rabe. In contrast, in YSb [see Figs. 8(c) and (d)] this p-d hybridization is very weak. Thus, a strong p-d hybridization need not be a prerequisite for the energy gap formation in these ternary systems. In fact as discussed below, Ni d orbitals play a crucial role.

In ZrNiSn, the Ni d orbitals do two things. The hybridized Sn p-Zr d band with a large dispersion (band labeled 1 in Fig. 8(a), which starts from the Γ point with Γ_{12} symmetry at $\sim$0.5 eV and goes to ~ -2.5 eV at the X point with $X_{4'}$ symmetry) in ZrSn hybridizes strongly with Ni d orbitals and becomes the *lowest conduction* band (along ΓX with X_3 symmetry at the X point) in ZrNiSn [band labeled 1 in Fig. 9(a)]. In addition, the strongly hybridized Sn p-Zr d band (band labeled 2 in Fig. 8(a), which starts from $\sim$0.0 eV at Γ and goes to $\sim$0.1 eV at X) gets slightly modified. The energy of this band at the X point drops below that at the Γ point by about $\sim$0.5 eV [band labeled 2 in Fig. 9(a)]. The net effect is the formation of an indirect gap semiconductor with a gap of 0.50 eV, which agrees very well with the previous calculation.[2,19] The situation is completely different in YNiSb. The lowest Y d band, which has a large downward

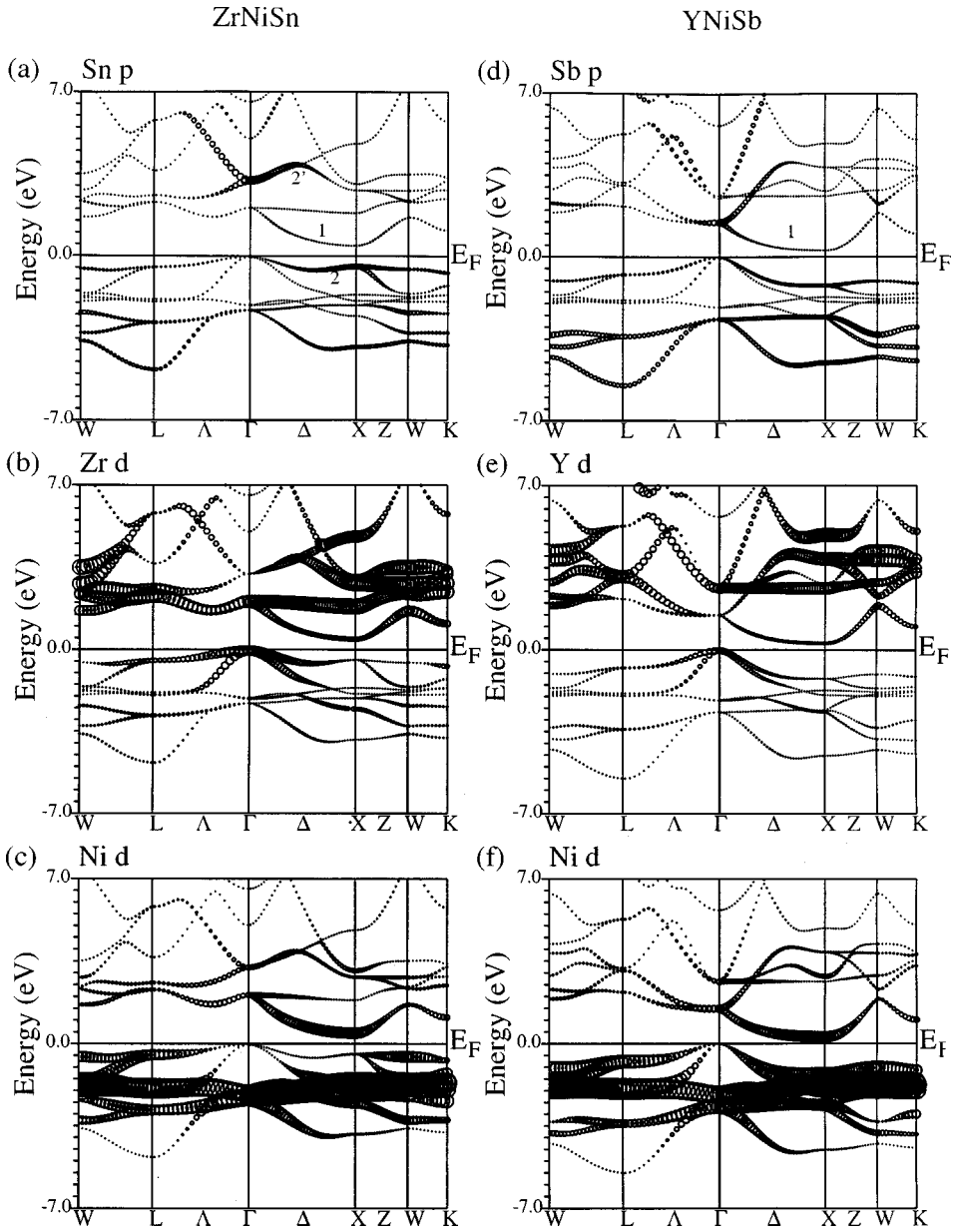

FIG. 9. Comparison of different angular characters between ZrNiSn (a), (b), and (c) and YNiSb (d), (e), and (f). The size of the circles is a measure of the strength of the angular character. Figures 9(a) and 9(d) give the *p* characters of Sn and Sb, Figs. 9(b) and 9(c) give the *d* characters of Zr and Y, respectively, and Figs. 9(c) and 9(e) give the *d* character of Ni.

dispersion going from Γ to X [band labeled 1 in Fig. 8(c)] strongly hybridizes with a Ni *d* band and somewhat weakly with Sb *p* band. This hybridization pushes the conduction band bottom at the X point above the valence band top at the Γ point [see band labeled 1 in Fig. 9(c)]. The net result is a formation of an indirect narrow gap semiconductor, but in this case the gap is 0.28 eV, about a factor of two smaller than that in the isoelectronic compound ZrNiSn. In spite of the basic differences in the nature of bonding, the energy band structure in the neighborhood of the Fermi energy is remarkably similar in ZrNiSn and YNiSb. There are, however, quantitative differences in the dispersion of the top of the valence band along the ΓX and ΓL directions between these two systems, which should reflect in their transport properties.

Recently Uher *et al.*[20] have studied the transport properties of ZrNiSn and related compounds. They have estimated the effective mass of the states near the bottom of the conduction band and find that it is about 2-3 times m_e, the free-electron mass. We have calculated the effective masses associated with the conduction-band minimum (at the X point) and find it to be highly anisotropic. Along the $X\Gamma$ direction the effective mass is about $10m_e$, whereas along the two other orthogonal directions, it is nearly m_e. Thus, we expect that the average transport mass will be about $(10)^{1/3}m_e$, which is consistent with Uher *et al.*'s finding. This might explain why the observed room-temperature electronlike thermoelectric coefficient in ZrNiSn is large.[20] A similar situation also occurs in YNiSb where the heavy electron mass along the $X\Gamma$ direction is a factor of two larger. If YNiSb can be doped *n* type, it should also show a large negative thermopower at room temperature. We find that the effective hole masses in ZrNiSn are large which suggests that *p*-doped ZrNiSn should show large positive ther-

mopower at room temperature. In contrast, the hole effective masses in YNiSb are not as large and therefore hole-doped YNiSb should not show large thermopower at room temperature.

IV. SUMMARY AND DISCUSSION

In summary, present FP-LAPW calculations within DFT and generalized gradient corrections yield the following results: When the *f* levels of the rare-earth atoms lie far away from the Fermi level, the systems are indirect narrow-gap semiconductors. Examples are the La, Lu, and Y compounds. The origin of the gap can be identified primarily with the interaction between the Ni *d* orbitals and the *d* orbitals of Y and rare-earth atoms, somewhat different from the origin of the gap formation in ZrNiSn systems[2,19] where hybridization between Sn *p* and Zr *d* orbitals also played a crucial role. The Ni *d* levels lie mainly below the Fermi level but push the conduction band (which becomes a hybridized Y-*d* and Ni-*d*) along the ΓX direction so that there is a gap between the top of the valence band (at Γ) and the bottom of the conduction band (at *X*). In contrast to the previous calculations,[4] we do not find any *M* valence *s* character below the Fermi energy. The calculated effective masses associated with the lowest conduction band are quite large and are consistent with the transport measurements in ZrNiSn.[20]

For the Yb system, the *f* levels come very close to the Fermi energy and there is strong (*f*-*p*) hybridization. The band structure is qualitatively similar to that of YbPtBi.[7] The density of states near the Fermi level is quite large due to the *f*-level contribution. The adequacy of LDA in describing narrow bands, such as *f* bands in rare earth needs to be critically examined. The GGA does take into account to some extent the effect of density gradients in the exchange and correlation potential when the charge density is nonuniform. This may not however be enough and to get a proper description of the physics of the system one has to incorporate corrections beyond LDA and GGA arising from strong electron-electron interactions in narrow band systems. In a recent letter, Oppener *et al.*[8] discussed the Fermi-level pinning of the so-called massive electron state in YbPtBi. As discussed above, LDA calculations of McMullan and Roy[7] gave a narrow *f* peak in the DOS near the Fermi energy. However, the calculated DOS at the Fermi energy was an order of magnitude too small to explain the huge linear heat capacity seen in this system at low temperature.[21] Oppener *et al.* argued that the strong intrasite correlations associated with the *f* states of the Yb atom were not handled properly within LDA and its generalization to the magnetic systems, LSDA. They used a LSDA+*U* approach[22] instead, and found that most of the *f* component of the DOS got pushed down by about *U* ($\sim$5–6 eV), but a very narrow peak of *f* character appeared near the Fermi level. In fact, the Fermi energy was pinned to this very narrow *f* band. The net result was an increase in the DOS at the Fermi level and a corresponding increase in the calculated linear heat capacity at low temperature by a factor of 5–6 compared to the original LDA calculations. We expect that in YbNiSb a similar situation might arise and affect its properties at low temperatures. However, the width of this narrow correlation-induced peak can be strongly temperature dependent. We want to understand the physical ramifications of the LDA+*U* or LSDA+*U* calculations critically before applying this theory to the YbNiSb system.

ACKNOWLEDGMENTS

This work was partially supported by DARPA Grant No. DAAG55-97-1-0184. We thank Professor C. Uher for sending a copy of his manuscript prior to publication.

[1] F. G. Aliev, N. B. Brandt, V. V. Moschalkov, V. V. Kozyrkov, R. V. Skolozdra, and A. I. Belogorokhov, Z. Phys. B **80**, 353 (1990), and references therein; F. G. Aliev, Physica B **171**, 199 (1991); R. Kuentzler, R. Clad, G. Schmerber, and Y. Dossmann, J. Magn. Magn. Mater. **104-107**, 1976 (1992); H. Hohl, A. P. Ramirez, W. K. Fess, Ch. Thurner, Ch. Kloc, and E. Bucher, in *Thermoelectric Materials—New Directions and Approaches*, edited by T. M. Tritt *et al.*, MRS Symposia Proceedings No. 478 (Materials Research Society, Pittsburgh, 1997), p. 109.

[2] S. Ogut and K. M. Rabe, Phys. Rev. B **51**, 10 443 (1995).

[3] K. Takegahara and T. Kasuya, Solid State Commun. **74**, 243 (1990).

[4] A. K. Solanki, A. Kashyap, S. Auluck, and M. S. S. Brooks, J. Appl. Phys. **75**, 6301 (1994).

[5] S. K. Dhar, S. Ranakrishnan, R. Vijayaraghaban, G. Chandra, K. Satoh, J. Itoh, Y. Onuki, and K. A. Gschneider, Jr., Phys. Rev. B **49**, 641 (1994).

[6] I. Karla, J. Pierre, and R. V. Skolozdra, J. Alloys Compd. **265**, 42 (1998).

[7] G. J. McMullen and M. P. Roy, J. Phys.: Condens. Matter **4**, 7095 (1992).

[8] P. M. Oppener, V. N. Antonov, A. N. Yaresco, A. Ya Perlov, and H. Eschrig, Phys. Rev. Lett. **78**, 4079 (1997).

[9] S. Sportouch, P. Larson, M. Bastea, P. Brazis, J. Ireland, C. R. Kannewarf, S. D. Mahanti, C. Uher, and M. G. Kanatzidis, in *Thermoelectric Materials 1998, The Next Generation Materials for Small-Scale Refrigeration and Power Generation Applications*, edited by T. M. Tritt *et al.*, MRS Symposia Proceedings No. 545 (Materials Research Society, Pittsburgh, 1999), p. 421.

[10] There have been some suggestion [see G. Mahan and J. O. Sofo, Proc. Natl. Acad. Sci. USA **93**, 7436 (1996)] that if *f* levels lie close to the Fermi energy, the systems can exhibit large thermoelectric response.

[11] P. Villars and L. D. Calvert, *Pearson's Handbook of Crystallographic Data for Intermetallic Phases* (American Society of Metals, Metals Park, OH, 1985).

[12] D. Singh, *Plane Waves, Pseudopotentials, and the LAPW Method* (Kluwer Academic, Boston, 1994).

[13] P. Hohenberg and W. Kohn, Phys. Rev. **136**, B864 (1964); W. Kohn and L. Sham, *ibid.* **140**, A1133 (1965).

[14] J. P. Perdew, K. Burke, and M. Ernzerhof, Phys. Rev. Lett. **77**, 3865 (1996).

[15] P. Blaha, K. Schwarz, and J. Luitz, WIEN 97 (Vienna University of Technology, Vienna, 1997).

[16] D. D. Koelling and B. Harmon, J. Phys. C **10**, 3107 (1977); P. Novak (unpublished).

[17] A. Hasegawa, J. Phys. C **13**, 6147 (1980).

[18] E. K. R. Runge, R. C. Albers, N. E. Christensen, and G. E. Zwicknagl, Phys. Rev. B **51**, 10 375 (1995).

[19] Our analysis of the origin of gap formation in ZrNiSn differs in one essential way from that presented by Ogut and Rabe (Ref. 2) (OR) in regard to the role of Ni insertion into the fcc ZrSn. OR argued that the role of Ni insertion was primarily that of local symmetry breaking, which allowed (leading to uncrossing) previously forbidden mixing between Zr d_{xy} band (along ΓX-001 direction) and the bands derived from Zr d_{3z2-r2} and Sn p_z orbitals. The Ni d component of the conduction band was claimed to be very small. While we find Ni-induced symmetry breaking to be important, we also find a strong mixing of the Ni and Zr d orbitals. The lowest conduction band along the ΓX direction in ZrNiSn has a very large Ni d character [see Fig. 9(c)] and in particular the conduction band minimum at the X point (X_3 symmetry) has both Ni and Zr d characters in contrast to the findings of OR who claim this point to be of primarily Zr d character.

[20] C. Uher, J. Yang, S. Hu, D. T. Morelli, and G. P. Meisner, Phys. Rev. B **59**, 8615 (1999).

[21] Z. Fisk, P. C. Canfield, W. P. Beyerman, J. D. Thompson, M. F. Hundley, H. R. Ott, E. Fedder, M. B. Maple, M. A. de la Tora, P. Visani, and C. L. Seaman, Phys. Rev. Lett. **67**, 3310 (1991).

[22] V. I. Anisimov, I. V. Solovyev, M. A. Kortin, M. T. Czyzyk, and G. A. Sawatzky, Phys. Rev. B **48**, 16 929 (1993).